Macromolecules

ARTICLE

pubs.acs.org/Macromolecules

Using Hydrogen-Bonding Interactions To Control the Peptide Secondary Structures and Miscibility Behavior of Poly(L-glutamate)s with Phenolic Resin

Shiao-Wei Kuo* and Chi-Jen Chen

Department of Materials and Optoelectronic Science, Center for Nanoscience and Nanotechnology, National Sun Yat-Sen University, Kaohsiung, Taiwan

Supporting Information

ABSTRACT: We synthesized three low-molecular-weight poly(glutamate)s—poly(γ-methyl L-glutamate) (PMLG), poly(γ-ethyl L-glutamate) (PELG), and poly(γ-benzyl L-glutamate) (PBLG)—through living ring-opening polymerization of their α-amino acid-*N*-carboxyanhydride derivatives and then blended them with phenolic resin to control the secondary structures of these polypeptides. Each of the three binary blends exhibited a single glass transition temperature (differential scanning calorimetry) and a single-exponential decay of proton spin−lattice relaxation times in the rotating frame [$T_{1\rho}^{H}$; solid state nuclear magnetic resonance (NMR) spectroscopy], characteristic of a miscible system. The strength of the interassociative interactions depended on the nature of the hydrogen bond acceptor groups, increasing in the order phenolic/PELG > phenolic/PMLG > phenolic/PBLG, as evidenced through analyses using Fourier transform infrared (FTIR) spectroscopy and the Painter−Coleman association model. The fractions of α-helical conformations (measured using FTIR and solid-state NMR spectroscopy) of PMLG and PELG decreased initially upon increasing the phenolic content but increased thereafter; in contrast, the fraction of α-helical conformations of PBLG increased continuously upon increasing the phenolic contents. Using variable-temperature infrared spectroscopy to investigate the changes in the conformations of the secondary structures of the peptide segments in these three binary blends, we found that the α-helical conformation in these three blend systems correlated strongly with the rigidity of side-chain groups, the strength of the intermolecular hydrogen bonding with the phenolic resin, the compositions of phenolic resin, and the temperature. More interestingly, the content of α-helical conformations of the polypeptides in these phenolic/PBLG blends increased upon increasing the temperature.

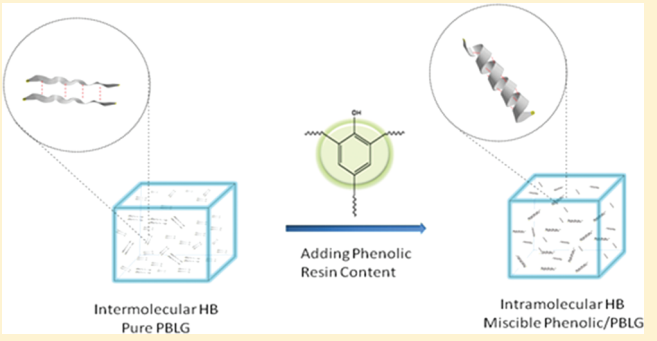

INTRODUCTION

The secondary structures of peptide chains influence the formation of well-defined tertiary structure of proteins.[1] Polypeptides form hierarchically ordered structures containing α-helices, which can be regarded as a rigid rods stabilized through intramolecular hydrogen-bonding interactions, and β-sheets, stabilized by intermolecular interactions, as fundamental secondary motifs.[2] From a synthetic point of view, the α-helical structures of polypeptides [e.g., poly(γ-benzyl L-glutamate) (PBLG)] cause them to behave as rigid-rod-like polymers in solution and in the solid state,[3−5] providing unique bulk (e.g., thermotropic liquid crystalline ordering[6,7]) and solution (thermoreversible gelation[8−10]) behavior. The β-sheet secondary structure is also an important feature in the development of several neurodegenerative disorders (e.g., prion diseases).[11] As a result, conformational studies of model polypeptides are important steps toward mimicking the biological activity of more-complex proteins.[12]

For several decades, most methods for synthesizing poly(peptide-*b*-non-peptide) (rod/coil) block copolymers, with potential applications in tissue engineering and drug delivery, have followed nature's strategies for producing supramolecular bioactive assemblies.[13−24] The non-peptide blocks have often been used as macroinitiators; for example, polystyrene,[20] poly(ethylene oxide),[25] poly(dimethylsiloxane),[26,27] poly(ε-caprolactone),[28] poly(*N*-isopropylacrylamide),[29] poly(butadiene),[30] poly(isoprene),[31] poly(2-ethyl-2-oxazoline),[32] and polyfluorene.[33] Klok et al. reported that the Fourier transform infrared (FTIR) spectra of poly(styrene-*b*-γ-benzyl L-glutamate) (PS-*b*-PBLG) copolymers revealed significant stabilization of the α-helical secondary structure relative to those of the corresponding PBLG oligomers.[20] We have previously combined the well-defined macromolecular architectures of polyhedral oligomeric silsesquioxane (POSS) and PBLG to generate polymeric building blocks (POSS-*b*-PBLG), and we have incorporated POSS moieties at the chain ends of PBLG units to allow intramolecular hydrogen bonding to occur between the POSS and PBLG units, thereby enhancing the latter's α-helical conformations in the

Received: March 28, 2011
Revised: July 25, 2011
Published: August 18, 2011

solid state.[35−37] The synthesis of diblock copolymers is, however, a difficult and time-consuming method for varying the secondary structure of a polypeptide. From practical and economical points of view, physical blending is a simpler and more effective method of modifying polypeptides and other useful materials, with greater versatility and flexibility, than is the development of new polymers.[38−42]

Here, we report that the secondary structures of polypeptides can be altered through blending with other random-coil non-peptide oligomers, mediated by hydrogen-bonding interactions. Painter et al. used infrared spectroscopy (IR) and optical microscopy to study the phase behavior of blends of three polyglutamates [poly(γ-methyl L-glutamate) (PMLG), poly(γ-ethyl L-glutamate) (PELG), and PBLG] with the random-coil polymer poly(vinylphenol) (PVPh).[38] In that study, each of these three polypeptides with flexible side chains adopted an α-helical rigid-rod conformation because of its high molecular weights: PMLG (46 000 g/mol), PELG (160 000 g/mol), PBLG (248 000 g/mol), and PVPh (9000−11 000 g/mol).[2,43] The presence of intermolecular hydrogen bonds between the C═O groups on the side chains of PMLG and PELG and the OH groups of PVPh, but not between PBLG and PVPh, indicated that the latter system was immiscible and phase-separated.[38] At a low degree of polymerization (e.g., DP < 18 for PBLG), both secondary structures (α-helix, β-sheet) are present; when the DP increases, however, the α-helical secondary structure is favored.[2,43] In addition, high DPs cause the entropic term to become small, thereby decreasing the miscibility of polymer blend systems.[44] As a result, for this study we synthesized three low-molecular-weight (both α-helical and β-sheet secondary structures) polyglutamates (PMLG, PELG, and PBLG) through living ring-opening polymerization of α-amino acid-*N*-carboxyanhydride (NCA) derivatives and then blended them with phenolic resin (M_n = 500 g/mol) as a means of altering their secondary structures. In addition, we expected the various side-chain groups of PMLG, PELG, and PBLG to affect the secondary structures by influencing the degrees of hydrogen bonding with the phenolic resin. We have used differential scanning calorimetry (DSC), FTIR spectroscopy, and solid-state nuclear magnetic resonance (NMR) spectroscopy to investigate the miscibility behavior, hydrogen-bonding interactions, and secondary structures of these phenolic/polyglutamates blends. We have also used variable-temperature IR spectroscopy to investigate the conformational changes that occur within the polypeptide segments upon blending with phenolic resin.

EXPERIMENTAL SECTION

Materials. Butylamine was purchased from Tokyo Kasei Kogyo, Japan. γ-Methyl L-glutamate *N*-carboxyanhydride, γ-ethyl L-glutamate *N*-carboxyanhydride, and γ-benzyl L-glutamate *N*-carboxyanhydride monomers were prepared according to a literature procedure[45] and stored at −30 °C. The phenolic was synthesized via a sulfuric acid-catalyzed condensation reaction, producing an average molecular weight (M_n) of 500, using a procedure described previously.[46]

PMLG, PELG, and PBLG. In a typical experiment, the NCA monomer (2 g) was weighed in a glovebox under pure Ar, placed in a flame-dried Schlenk tube, and dissolved in anhydrous *N*,*N*-dimethylformamide (DMF, 40 mL). The solution was stirred for 10 min, and then butylamine (50 μL) was added using a N_2-purged syringe. After stirring the solution for 40 h at room temperature, the polymer was recovered through precipitation in diethyl ether and dried under high vacuum.

Blend Preparations. Blends of phenolic/PMLG, phenolic/PELG, and phenolic/PBLG at various blend compositions were prepared through solution casting. A DMF solution containing 5 wt % of the polymer mixture was stirred for 6−8 h, and then the solvent was evaporated slowly at 50 °C for 1 day. The film of the blend was then dried at 80 °C for 2 days to ensure total removal of residual solvent.

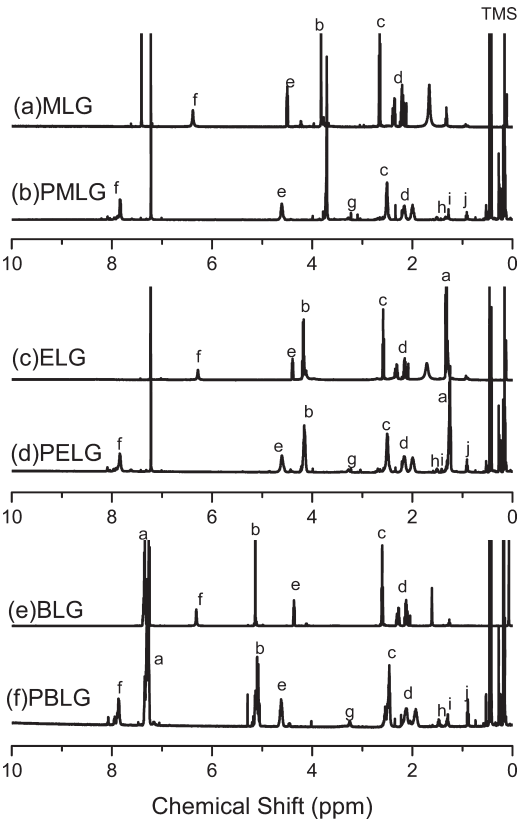

Figure 1. ^{1}H NMR spectra of the (a) MLG, (c) ELG, and (e) BLG monomers in $CDCl_3$ and the (b) PMLG, (d) PELG, and (f) PBLG polypeptides in $CDCl_3$ containing 15 wt % TFA.

Characterization. ^{1}H NMR spectra were recorded at room temperature using a Bruker AM 500 (500 MHz) spectrometer, with the residual proton resonance of the deuterated solvent as the internal standard. High-resolution solid-state NMR spectra were recorded at room temperature using a Bruker DSX-400 spectrometer operated at resonance frequencies of 399.53 and 100.47 MHz for ^{1}H and ^{13}C nuclei, respectively. The ^{13}C CP/magic angle sample spinning (MAS) spectra were measured with a 3.9 μs 90° pulse, a 3 s pulse delay time, a 30 ms acquisition time, and 2048 scans. All NMR spectra were recorded at 300 K using broad-band proton decoupling and a normal cross-polarization pulse sequence. An MAS rate of 5.4 kHz was used to avoid absorption overlapping. The proton spin−lattice relaxation time in the rotating frame ($T_{1\rho}^{H}$) was determined indirectly via carbon observation using a 90°−τ−spin lock pulse sequence prior to cross-polarization. The data acquisition was performed via ^{1}H decoupling and delay times (τ) ranging from 0.1 to 12 ms with a contact time of 1.0 ms. Thermal analysis through DSC was performed using a DuPont 910 DSC-9000 controller operated at a scan rate of 10 °C/min over a temperature range from −50 to +120 °C under a N_2 atmosphere. FTIR spectra of the polymer films were recorded using the conventional KBr disk method. FTIR spectra were recorded using a Bruker Tensor 27 FTIR spectrophotometer; 32 scans were collected at a spectral resolution of 1 cm^{-1}. Because polymers containing OH groups are hygroscopic, pure N_2 gas was used to purge the spectrometer's optical box to ensure dry sample films. IR spectra of samples at elevated temperatures were recorded using a cell mounted within the temperature-controlled compartment of the spectrometer.

Scheme 1. Syntheses of PMLG, PELG, and PBLG, Using Butylamine as the Initiator

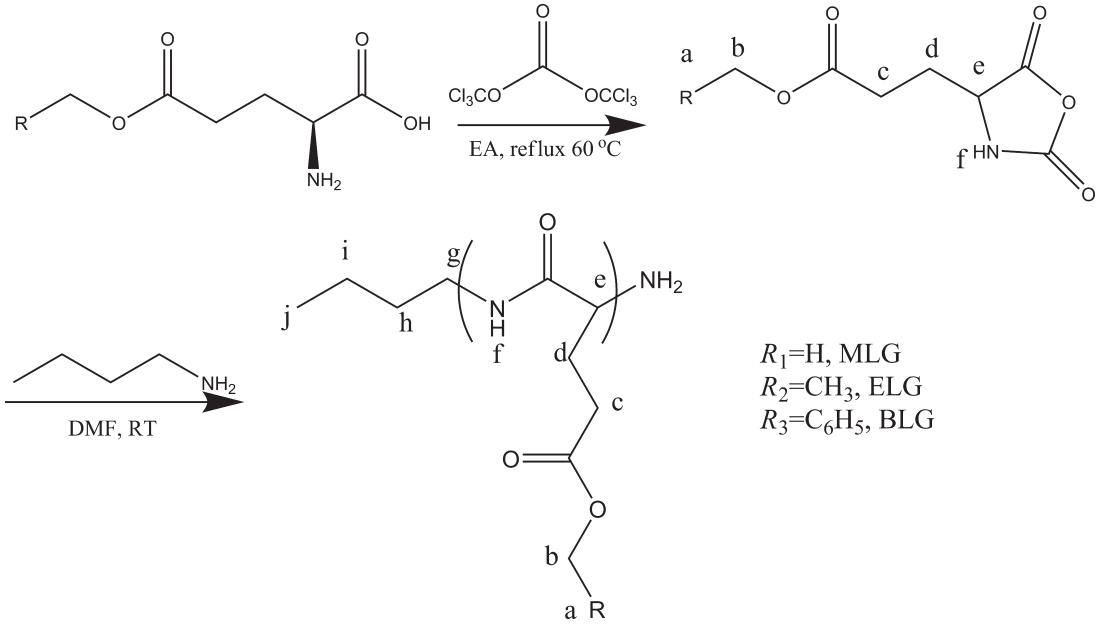

RESULTS AND DISCUSSION

Synthesis of PMLG, PELG, and PBLG. Figure 1 presents the ^{1}H NMR spectra of the MLG, ELG, and BLG monomers in $CDCl_3$. We assign each singlet at 6.4 ppm to the proton on the ring nitrogen atom; the signals at 3.83, 4.18, and 5.12 ppm to the COOC**H**$_2$R protons of MLG, ELG, and BLG, respectively; the multiplets between 2.0 and 2.6 ppm to the alkyl CH_2 protons; and, for BLG, the signals at 7.31−7.38 ppm to the benzyloxy ring protons. Figure 1 also displays the ^{1}H NMR spectra of PMLG, PELG, and PBLG in $CDCl_3$ containing 15% TFA. The signals of the protons on the nitrogen atoms of PMLG, PELG, and PBLG resonated at 7.9 ppm (singlet); the signals of the butyl groups were located at 0.9 ($CH_3C_3H_6$, triplet), 1.3 ($CH_3CH_2C_2H_4$, multiplets), 1.5 (C_2H_5-CH_2CH_2, multiplets), and 3.2 ppm ($C_3H_7CH_2NH$, triplet), and for PBLG, the signals of the aromatic protons appeared as multiplets at 7.31−7.38 ppm. Scheme 1 presents assignment for all of the other signals in the ^{1}H NMR spectra of PMLG, PELG, and PBLG. We determined the molar masses of PMLG, PELG, and PBLG from their ^{1}H NMR spectra using the equation[47,48]

$$M_{n,\,PLG} = \frac{I_b M_{LG}}{I_g} + M_{butylamine}$$

where I_b and I_g are intensities of the signals of the methylene protons *b* on the side chains of PMLG, PELG, and PBLG and the methylene protons *g* of the butylamine initiator, respectively. $M_{butylamine}$ is the molar mass of the butylamine initiator. Table 1 lists the DPs of PMLG, PELG, and PBLG as determined using ^{1}H NMR spectroscopy.

Figure 2 displays FTIR spectra of the MLG, ELG, and BLG monomers and their corresponding polymers, recorded at room temperature. Two typical C═O stretching bands—at 1873 and 1789 cm^{-1}, corresponding to the C═O units *a* and *b*, respectively—confirm the formation of the NCA ring;[49] the C═O stretching bands at 1711 cm^{-1} correspond to free C═O units *c* of the MLG, ELG, and BLG NCA monomers. After ring-opening polymerization of the NCA monomers, FTIR spectra revealed the absence of the absorbances from the C═O groups *a* and *b* of the NCA rings and the appearance of new absorbance at 1655, 1627 (*d*), and 1543 cm^{-1} (*e*), representing amide bonds in the polymer backbone.[49] Our ^{1}H NMR and FTIR spectroscopic analyses confirmed that the successful syntheses of PMLG, PELG, and PBLG.

Table 1. Self- and Interassociation Equilibrium Constants and Thermodynamic Parameters of the Phenolic/PMLG, Phenolic/PELG, and Phenolic/PBLE Blends at 25 °C[a]

					equilibrium constant		
polymer	*V*	M_w	Δ	DP	K_2	K_B	K_A
phenolic	84.0	105	12.0	6	23.3	52.3	
PMLG	105.5	143	11.5	10			30.0
PELG	122.0	157	11.0	9			50.0
PBLG	165.9	219	11.2	7			9.0

[a] *V* = molar volume (mL/mol),[43] M_w = molecular weight (g/mol), δ = solubility parameter (cal/mL)$^{1/2}$,[43] DP = degree of polymerization, K_2 = dimer self-association equilibrium constant, K_B = multimer self-association equilibrium constant, and K_A = interassociation equilibrium constant.

Figure 3 presents scale-expanded FTIR spectra of the C═O and amide stretching regions of PMLG, PELG, and PBLG, recorded at room temperature. We split the C═O and amide stretching frequencies of these three polypeptides split into four bands: at 1734−1741, 1690−1695, 1653−1656, and 1623−1627 cm^{-1}, corresponding to the free C═O groups (on the side chains) and the random coil, α-helical, and *β*-sheet secondary structures of the polypeptides, respectively.[2] These four bands fitted well to the Gaussian function; Figure 3 displays typical examples of the separation. The fractions of α-helical secondary structures of the polypeptides were similar (PMLG: 42.5%; PELG: 51.1%; PBLG: 51.2%). In this manner, we could readily distinguish the influence of each of the side chain groups of PMLG, PELG, and PBLG on the

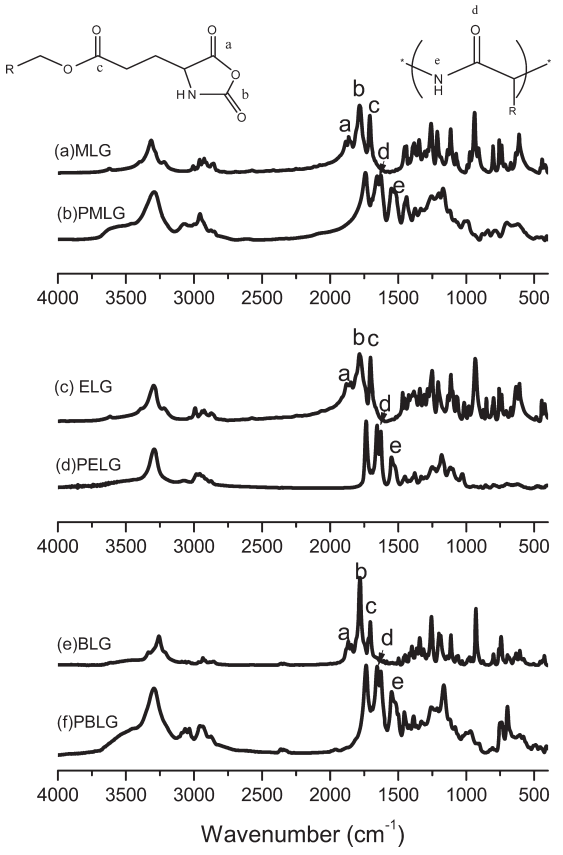

Figure 2. FTIR spectra of the (a) MLG, (c) ELG, and (e) BLG monomers and the (b) PMLG, (d) PELG, and (f) PBLG polypeptides at room temperature.

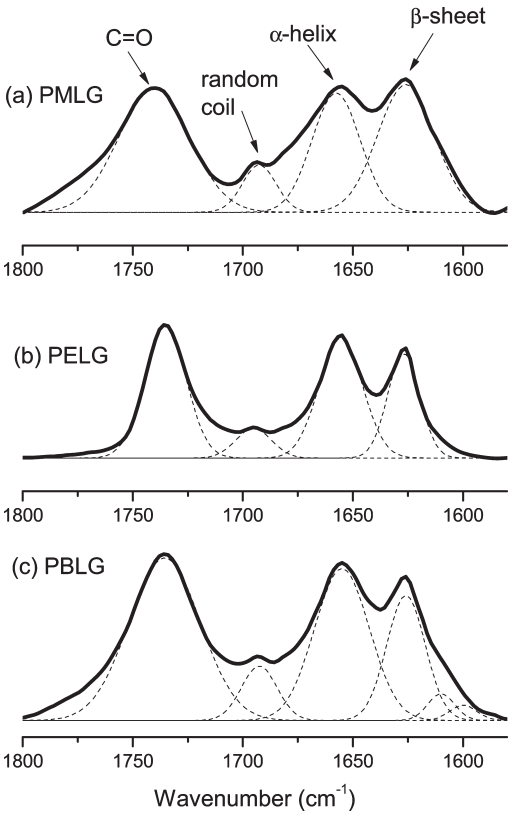

Figure 3. Curve fitting of the signals in the FTIR spectra of (a) PMLG, (b) PELG, and (c) PBLG.

secondary structure, mediated through hydrogen bonding with the phenolic resin.

Thermal Analyses of Polymer Blends. Thermal characterization of polymer blends is a well-known method for determining the miscibility of polymer blends. Some miscible blends can show a dual glass temperature with a relatively large T_g difference between two homopolymers with weak intermolecular interactions.[50] In this study, the values of T_g of polypeptides having rigid objects with well-defined secondary structures (helices, sheets) were difficult to observe.[51] Previous studies reported that pure phenolic, PMLG, PELG, and PBLG were +55, −11, −13, and +18 °C, respectively.[38,52] The T_g difference is not large, and the hydrogen-bonding interaction is strong as evidenced by FTIR analyses in this study that will be discussed in next section. As a result, the miscibility of any two polymers in the amorphous state is characterized by the presence of a single glass transition temperature (T_g).

Figure 4 presents the second heating runs in our DSC analyses of phenolic resin blends with PMLG, PELG, and PBLG at various compositions; all three blend systems exhibit a single glass transition temperature over the entire range of compositions, indicating that they were fully miscible blends exhibiting a homogeneous amorphous phase. For PMGL and PELG, the characteristics of the blends with phenolic resin were in general agreement with those of their blends with the PVPh homopolymer. In contrast, the PVPh/PBLG blends were immiscible and phase-separated, presumably because of the (i) much lower molecular weights of the PBLG (2000 g/mol) and the hydrogen

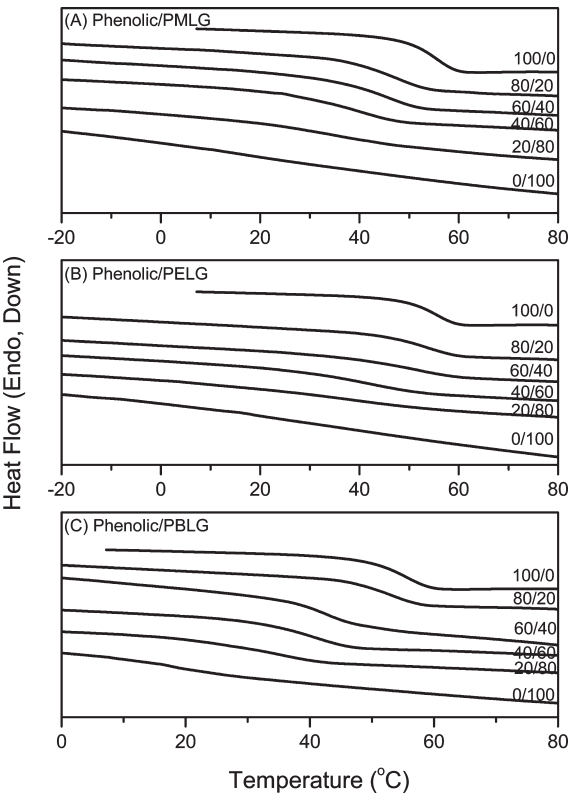

Figure 4. DSC traces (second heating run) of (A) phenolic/PMLG, (B) phenolic/PELG, and (C) phenolic/PBLG blends.

dx.doi.org/10.1021/ma200721e |*Macromolecules* 2011, 44, 7315–7326

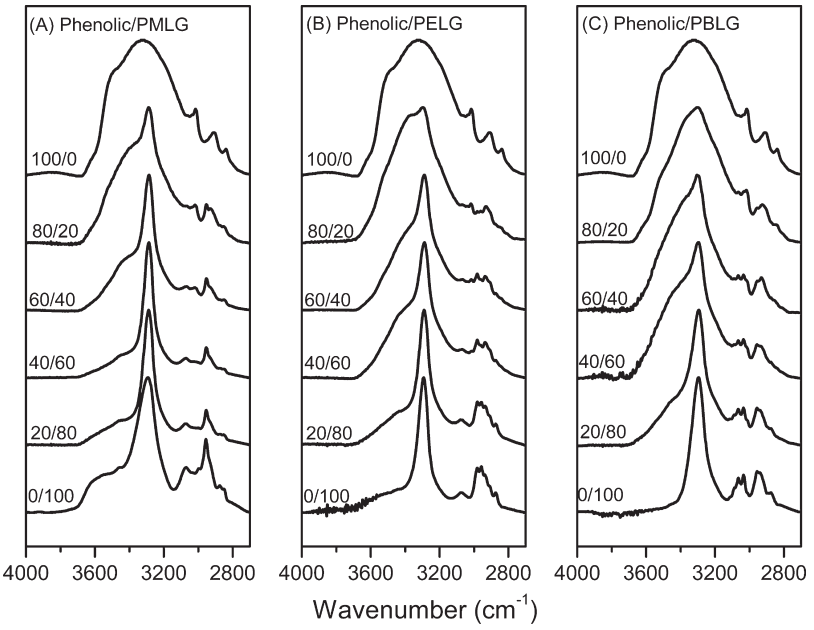

Figure 5. FTIR spectra (4000−2700 cm^{-1}) recorded at room temperature for the (A) phenolic/PMLG, (B) phenolic/PELG, and (C) phenolic/PBLG blends.

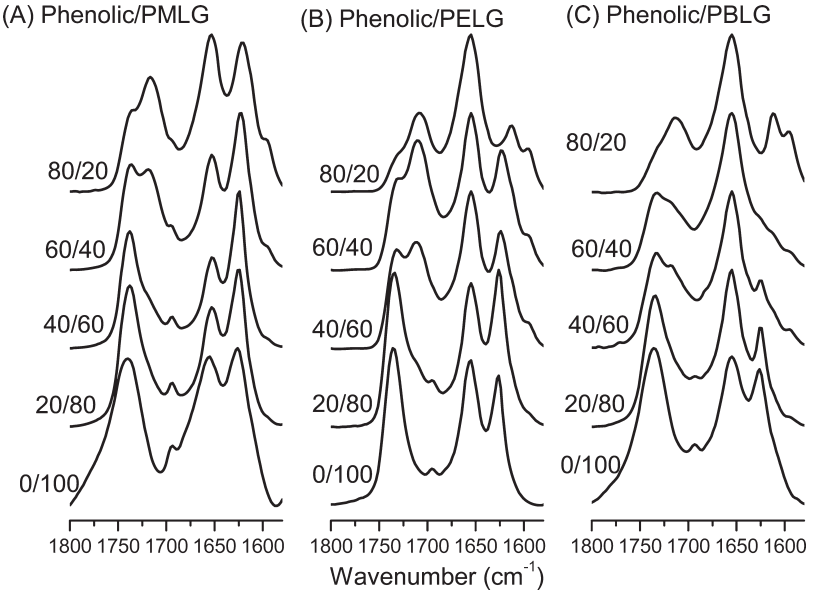

Figure 6. FTIR spectra (1800−1580 cm^{-1}) recorded at room temperature for the (A) phenolic/PMLG, (B) phenolic/PELG, and (C) phenolic/PBLG blends.

bond donor polymer [500 g/mol (phenolic)] used in this study, relative to those [248 000 (PBLG) and 11 000 (PVPh) g/mol] used previously, with the lower DPs increasing the entropic terms and thereby enhancing the miscibility of the polymer blend system,[44] and (ii) stronger interassociation hydrogen bonding of PBLG with the phenolic resin than with the PVPh,[53,54] as has been reported in previous studies,[55,56] contributing significantly to the enthaplic term.[44]

Hydrogen-Bonding Interactions and Conformations of the Peptide Segments after Blending with Phenolic Resin. IR spectroscopy can provide information regarding the specific interactions between polymers, both qualitatively and quantitatively. The OH stretching range in an IR spectrum is sensitive to the degree of hydrogen bonding. Figure 5 displays FTIR spectra (in the range 2700−4000 cm^{-1}) of phenolic/PMLG, phenolic/PELG, and phenolic/PBLG blends, recorded at room temperature. The spectrum of pure phenolic features two distinct bands in the OH stretching region: a very broad band centered at 3320 cm^{-1} representing the wide distribution of hydrogen-bonded OH groups and a sharp band at 3525 cm^{-1} representing the free OH groups. For the pure polypeptides, we observe a sharp band at 3290 cm^{-1}, representing NH stretching (primary amine) vibrations of the polypeptides. The intensity of the signal for the free OH groups decreased upon increasing the

polypeptide content, as would be expected. Meanwhile, the broad signal of the hydrogen-bonded OH groups shifted to higher frequency upon increasing the polypeptide content, whereas the sharp band representing the NH stretching vibrations of the polypeptides remained unchanged. All these observed changes suggest a switch from strong intramolecular OH···OH (phenolic/phenolic) hydrogen bonds into weak intermolecular OH···C═O (phenolic/polypeptides) hydrogen bonds,[57,58] with no hydrogen-bonding interactions between OH groups of phenolic and the NH groups of the polypeptides.

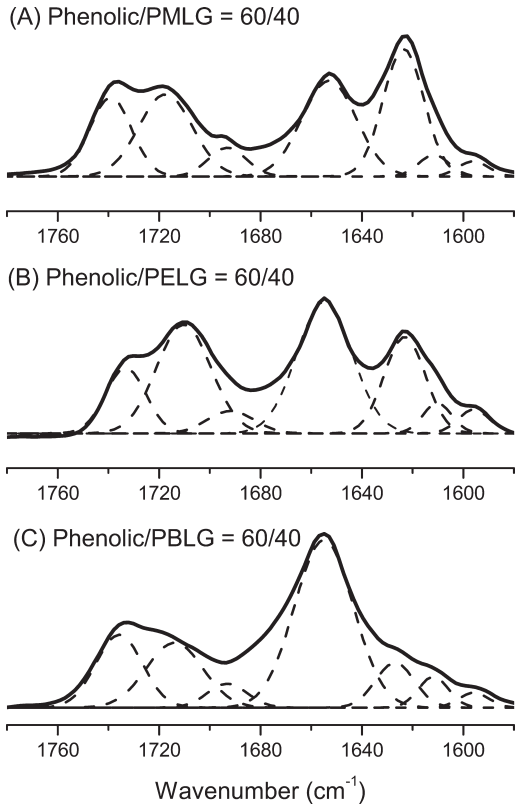

Figure 7. Curve fitting of the signals in the FTIR spectra of the (A) phenolic/PMLG = 60/40, (B) phenolic/PELG = 60/40, and (C) phenolic/PBLG = 60/40 blends.

We recorded FTIR spectra at room temperature to obtain information regarding the hydrogen-bonding interactions and secondary structures of the phenolic/PMLG, phenolic/PELG, and phenolic/PBLG blends (Figure 6). Analyzing these spectra using the second-derivative technique,[13] we observed seven major peaks, representing the free C═O groups (1734−1741 cm^{-1});[38] the hydrogen-bonded C═O groups of the side chains (1710−1720 cm^{-1});[38] the secondary structures of the amide I groups in random coil (1690−1695 cm^{-1}),[13] α-helical (1653−1656 cm^{-1}),[20−22] and β-sheet (1623−1627 cm^{-1})[20−22] conformations; and the stretching of benzene units (1610 and 1594 cm^{-1}). Here, we ignore the amide I group in random coil at 1640−1650 and 1660−1670 cm^{-1} since many bands were difficult to calculate the quantitative area fraction of secondary structures.[59] For deconvolution, we fitted a series of Gaussian distributions to quantify the fraction of each of the peaks (Figure 7). Table 2 and Figures 8 and 9 summarize the curve fitting data for the amide I groups of the β-sheet, α-helical, and random coil structures and for the free and hydrogen-bonded C═O units of the side chains.

Figure 8 displays the fraction of hydrogen-bonded C═O groups of PMLG, PELG, and PBLG plotted with respect to the phenolic content at room temperature; it indicates that the fraction of hydrogen-bonded C═O groups on the side chains of the polypeptides increased upon increasing the phenolic resin contents. Furthermore, the degree of hydrogen bond formation in the blends with phenolic resin increased in the order phenolic/

Table 2. Curve Fitting Data for the C═O and Amide Groups in the Phenolic/Polypeptide Blends at 25 °C

	carbonyl group in polypeptide				amide group in polypeptide					
	free C═O		H-bond C═O		random coil		α-helix		β-sheet	
blend	ν (cm^{-1})	A_f (%)	ν (cm^{-1})	A_f (%)	ν (cm^{-1})	A_f (%)	ν (cm^{-1})	A_f (%)	ν (cm^{-1})	A_f (%)
phenolic/PMLG										
0/100	1741	100		0	1693	13.5	1655	42.5	1626	44.0
20/80	1739	70.4	1720	29.6	1693	9.3	1653	41.1	1625	49.6
40/60	1739	61.3	1718	38.7	1693	8.0	1653	35.2	1625	56.8
60/40	1739	37.8	1718	62.2	1692	5.8	1653	39.6	1623	54.6
80/20	1738	28.3	1717	71.7	1692	4.9	1654	46.8	1623	48.3
phenolic/PELG										
0/100	1735	100		0	1695	14.7	1655	51.1	1627	34.2
20/80	1735	68.1	1713	31.9	1692	9.3	1655	48.8	1626	41.9
40/60	1733	43.1	1710	56.9	1692	6.2	1655	56.0	1623	37.8
60/40	1733	28.7	1709	71.3	1692	4.5	1655	59.1	1623	36.4
80/20	1733	17.6	1709	82.4		0	1655	100		0
phenolic/PBLG										
0/100	1736	100		0	1693	18.2	1655	51.2	1625	30.6
20/80	1735	74.5	1711	25.5	1690	12.6	1655	65.4	1625	22.0
40/60	1735	66.5	1712	33.5	1690	10.4	1655	74.0	1624	15.6
60/40	1734	58.2	1710	41.8	1691	5.2	1655	86.6	1625	8.2
80/20	1734	40.0	1712	60.0		0	1655	100		0

dx.doi.org/10.1021/ma200721e |*Macromolecules* 2011, 44, 7315–7326

PELG > phenolic/PMLG > phenolic/PBLG. Compared with the data for blending with the PVPh homopolymer, the phenolic/PMLG and phenolic/PELG exhibited trends similar to those for the intermolecular hydrogen bonding that occurred between PVPh and PMLG or PELG; the proportion of hydrogen-bonded C═O groups of PVPh/PBLG was, however, negligibly small in most of the compositions. In the phenolic/PBLG blends, we observed relatively higher fractions of hydrogen-bonded C═O groups of PBLG than we had found previously for the PVPh/PBLG blends. Therefore, we confirmed that the phenolic/PBLG blend was a miscible system due to the existence of intermolecular hydrogen bonds between the OH groups of the phenolic resin and the C═O groups of PBLG. Next, we determined the corresponding inter- and self-association equilibrium constants for these systems. The self-association constants of phenolic resin (K_2 = 23.3; K_B = 52.3) have been determined previously.[60] We determined the interassociation constants K_A directly using a least-squares fitting procedure based on the fraction of hydrogen-bonded C═O observed experimentally in the binary phenolic/PMLG, phenolic/PELG, and phenolic/PBLG blends; we obtained values of 30, 50, and 9, respectively. Table 1 lists all the parameters required by the Painter−Coleman association model[43] to estimate the thermodynamic properties for these polymer blends. The interassociation equilibrium constants and relative ratios of K_A/K_B increased in the order phenolic/PELG > phenolic/PMLG > phenolic/PBLG. Therefore, the chemical structure of the group accepting the hydrogen bonds has great impact on these values, as has been discussed in detail previously.[55,56]

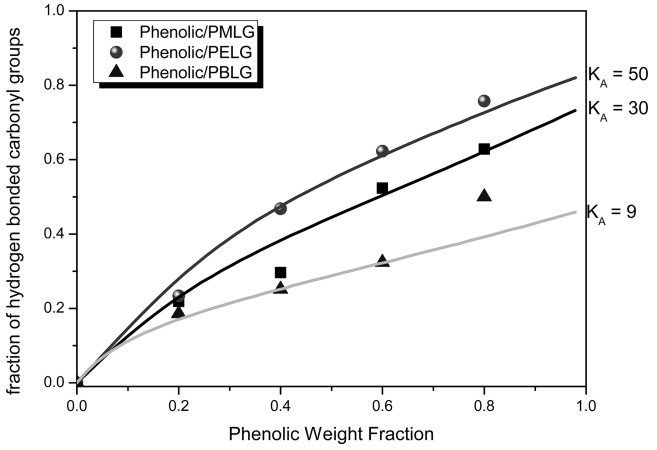

Figure 8. Fraction of hydrogen-bonding C═O groups of the polypeptides plotted with respect to the phenolic content and the corresponding interassociation equilibrium constants based on the Painter−Coleman association model.

Figure 9 summarizes the fractions of the secondary structures of PMLG, PELG, and PBLG with respect to the phenolic content, at room temperature. The fractions of the random coil structures of all three binary blends decreased upon increasing the phenolic content, indicating that the presence of the phenolic resin stabilized the secondary structures of the polypeptides. More interestingly, the fractions of the α-helical secondary structures of these three different polypeptides exhibited different trends upon increasing the phenolic resin content. For PMLG and PELG, the fractions of α-helical conformations decreased initially upon increasing the phenolic content but increased thereafter; in contrast, the fraction of the α-helical conformation of PBLG increased continuously upon increasing the phenolic content.

It has been reported that at a low DP of PBLG (DP < 18) both secondary structures (α-helix, β-sheet) are present, but when the DP increases, the α-helical secondary structure is favored.[2] In this study, we also observed both the α-helical and β-sheet conformations for the PBLG oligomer at a DP of 7; we found, however, that the content of α-helical conformations increased upon increasing the phenolic resin content. It has been proposed that stacking of the side-chain benzene rings of PBLG plays a role in stabilizing its various structures;[38] indeed, among all of our studied polypeptides, we found that PBLG at its lowest DP featured the highest content of α-helical conformations. Jeon et al. reported that the mobility of the side-chain groups of polyglutamates also affects the α-helical conformation.[61] Their experimental data revealed that longer flexible side chains

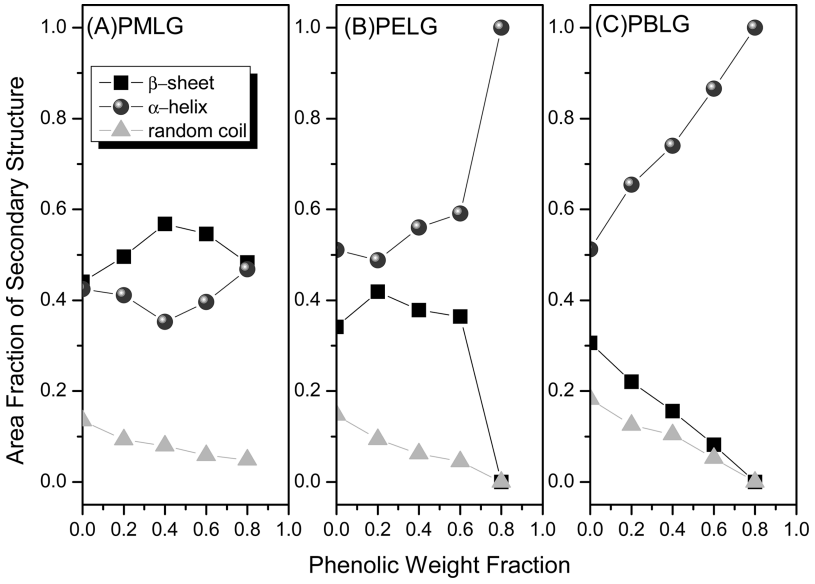

Figure 9. Secondary structures in the (A) phenolic/PMLG, (B) phenolic/PELG, and (C) phenolic/PBLG blends at various phenolic resin contents.

Scheme 2. Formation of α-Helical Conformations in Phenolic/PBLG Blends

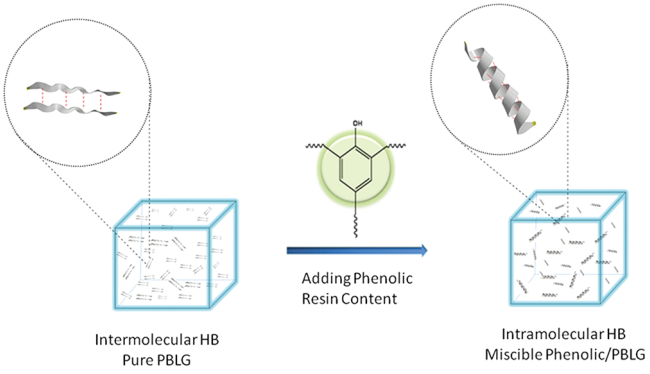

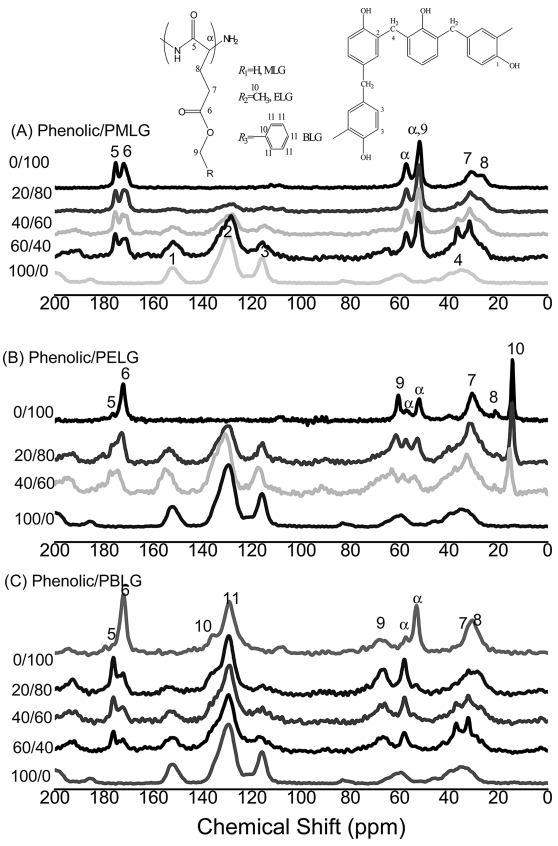

Figure 10. ^{13}C CPMAS spectra recorded at room temperature of the (A) phenolic/PMLG, (B) phenolic/PELG, and (C) phenolic/PBLG blends.

Table 3. Chemical Shifts (ppm) of the Signals in the ^{13}C CP/MAS/DD NMR Spectra of the Phenolic/Polypeptide Blends

	phenolic			
phenolic/PMLG	C-1	C-2	C-3	C-4
100/0	152.3	129.8	116.0	35.8
60/40	152.8	129.1	116.2	36.5
40/60	153.1	128.6	115.5	36.3
20/80	153.2	128.2	115.7	36.3

	PMLG					
	C-5	C-6	Cα	C-7	C-8	C-9
0/100	176.3	173.0	57.5/51.9	31.0	27.0	51.9
20/80	176.4	173.0	57.3/52.2	31.3	27.3	52.2
40/60	176.5	173.5	57.5/52.4	31.5	27.6	52.4
60/40	176.5	172.2	57.5/52.5	31.6	26.9	52.5

	phenolic			
phenolic/PELG	C-1	C-2	C-3	C-4
100/0	152.3	129.8	116.0	35.8
60/40	153.7	129.4	116.1	36.4
40/60	153.8	130.0	115.8	36.5

	PELG						
	C-5	C-6	Cα	C-7	C-8	C-9	C-10
0/100	176.3	172.1	57.8/52.5	31.1	21.7	60.9	14.7
40/60	176.6	172.7	57.8/53.1	32.2	21.3	61.8	14.9
60/40	175.9	172.8	57.4/52.8	31.7	20.5	62.0	14.3

	phenolic			
phenolic/PBLG	C-1	C-2	C-3	C-4
100/0	152.3	129.8	116.0	35.8
60/40	152.6	129.2	116.9	36.4
40/60	153.0	128.8	115.4	36.6
20/80	153.2	129.1	115.2	36.7

	PBLG							
	C-5	C-6	Cα	C-7	C-8	C-9	C-10	C-11
0/100	176.1	172.5	57.6/53.0	30.3	28.0	65.7	136.0	129.0
20/80	176.1	172.2	57.6/52.7	31.4	27.9	65.9	136.0	129.1
40/60	176.2	172.4	57.6/52.7	31.6	26.5	65.6	136.7	128.8
60/40	176.2	172.3	57.6/–	31.6	26.0	66.2	136.8	129.2

induced weaker hydrogen bonds forming between the C═O groups and the amide linkages of the α-helical conformation; a corollary is that rigid benzene rings might enhance hydrogen bonding between the C═O groups and the amide linkages of the α-helical conformation. In the phenolic/PBLG blend, hydrogen bonds formed between the C═O groups of PBLG and the OH groups of the phenolic resin; their presence would accentuate the rigidity of the side-chain groups of PBLG. Floudas et al. reported that suppression of the β-sheet secondary structure of polyalanine (PALa) occurs in PBLG-*b*-PALa copolymers as a result of a thermodynamic field created by the enthalpic interactions of unlike blocks.[12] It is well established that the α-helical and β-sheet conformations are stabilized by intra- and intermolecular hydrogen-bonding interactions, respectively. In the miscible phenolic/PBLG blend, intermolecular hydrogen bonding of the PBLG segments initially disrupted and then induced intramolecular hydrogen bonding between the PBLG segments upon increasing the phenolic resin content, as indicated in Scheme 2; as a result, the content of α-helical conformations increased upon increasing the phenolic resin content.

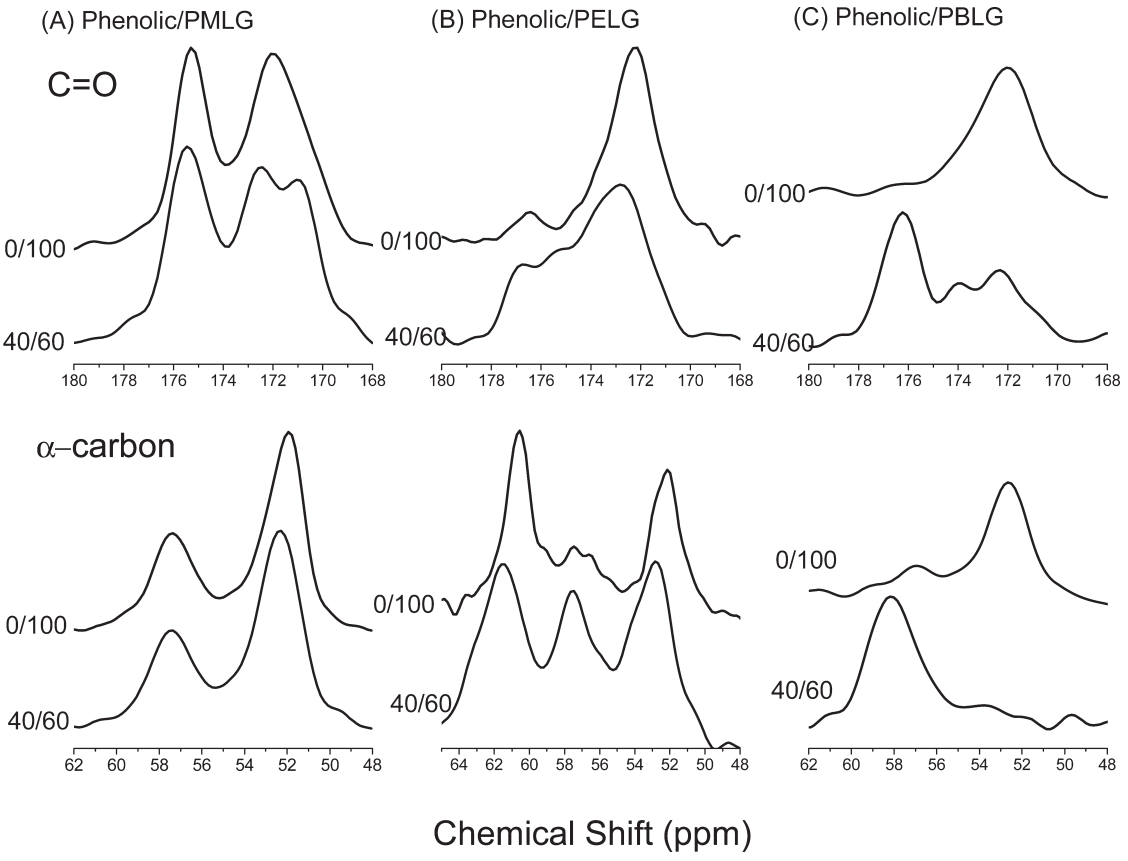

Figure 11. Scale-expanded solid-state ^{13}C NMR spectra (displaying signals for the C═O and C_α groups) of the (A) phenolic/PMLG, (B) phenolic/PELG, and (C) phenolic/PBLG blends.

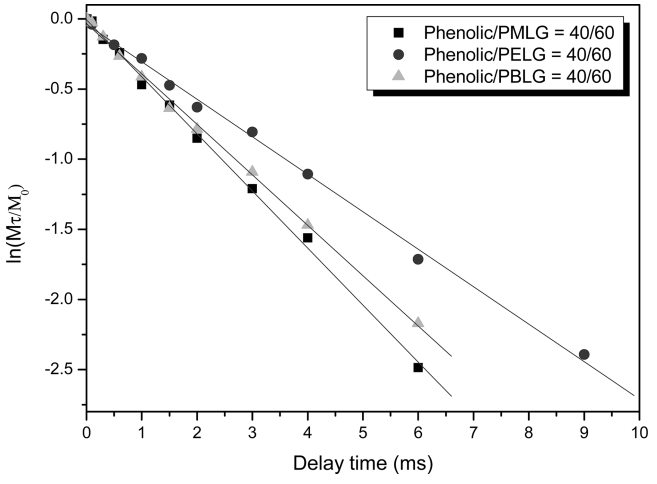

Figure 12. Semilogarithmic plots of the magnetization intensities of the signals at 115 ppm with respect to the delay time for the phenolic/PMLG, phenolic/PELG, and phenolic/PBLG blends.

In the phenolic/PMLG and phenolic/PELG blends, the fractions of α-helical conformations of PMLG and PELG decreased initially upon increasing the phenolic content (to 40 wt % for PELG and to 60 wt % for PMLG) but increased thereafter. This finding implies that, at lower phenolic contents, intermolecular hydrogen bonding of the PMLG and PELG segments increased to enhance the β-sheet conformations or that the random coils changed to β-sheet conformations. Because of the stronger hydrogen-bonding interactions in the phenolic/PELG than in the phenolic/PMLG blends, the PELG underwent an increase in its content of α-helical conformations at a relatively lower phenolic content. Therefore, the formation of α-helical conformations for polyglutamates is strongly dependent on the rigidity of the side chain groups, the strength of the intermolecular hydrogen bonds with phenolic resin, and the composition of the phenolic resin.

We could also identify the secondary structures of the polypeptides on the basis of distinctly different resonances in their solid-state NMR spectra. Figure 10 displays the ^{13}C CP/MAS spectra of the phenolic/PMLG, phenolic/PELG, and phenolic/PBLG blends at room temperature. The peak at 153.2 ppm represents the resonance of the phenolic carbon atom of pure phenolic (C-1).[62] The variations in this chemical shift of ca. 0.8, 1.5, and 0.7 ppm for the phenolic/PMLG, phenolic/PELG, and phenolic/PBLG blends, respectively, indicate the existence of intermolecular hydrogen bonding between the OH groups of the phenolic and the C═O groups of the polypeptide segments, with the strength of the intermolecular hydrogen bonds following the order phenolic/PELG > phenolic/PMLG > phenolic/PBLG, a trend that is similar to that deduced through FTIR spectroscopic analysis. Specific interactions in polymer blends can affect the chemical environments of neighboring molecules, resulting in upfield or downfield shifts in their resonances.[63−65] In addition, the different ^{13}C chemical shifts of the C_α and amide C═O resonances are related to the local conformations of the individual amino acid residues, characterized by the dihedral angles

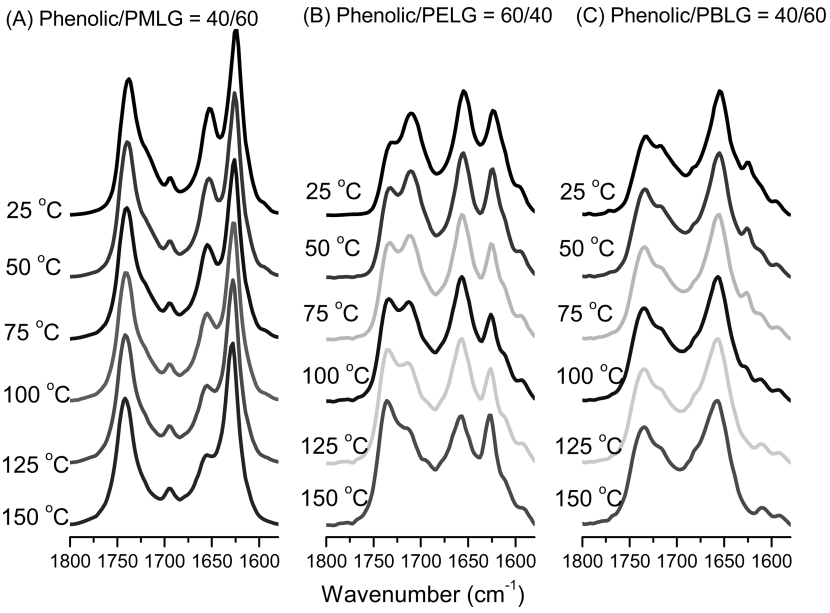

Figure 13. FTIR spectra of the (A) phenolic/PMLG = 40/60, (B) phenolic/PELG = 60/40, and (C) phenolic/PBLG = 40/60 blends, recorded at various temperatures.

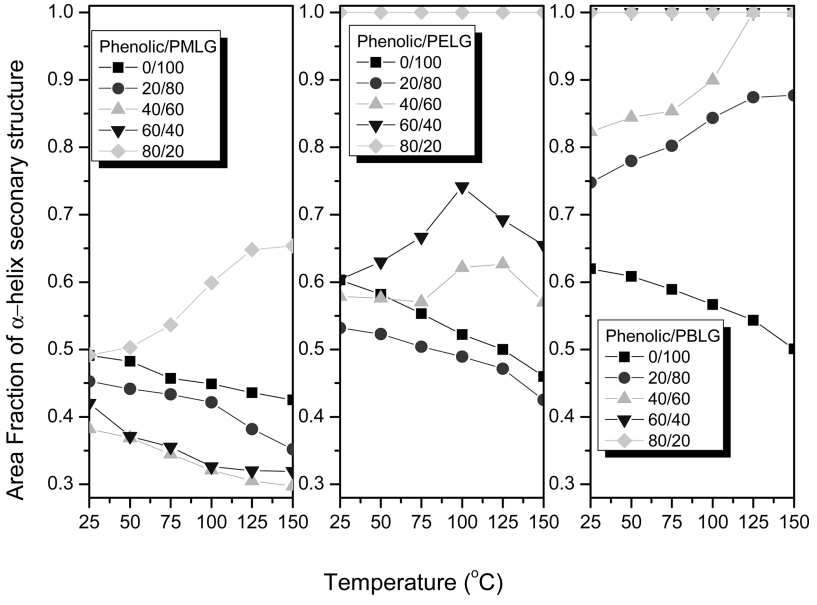

Figure 14. Summary of fractions of α-helical conformations of the (A) phenolic/PMLG, (B) phenolic/PELG, and (C) phenolic/PBLG blends at various temperatures.

and the types of intermolecular and intramolecular hydrogen-bonding interactions.[66,67] In the case of polyglutamate homopolymers, the side chains can stabilize the α-helical secondary structure; correspondingly, the chemical shifts of the C_α and amide C═O resonances appear at 57.5 and 176 ppm. In the β-sheet conformation, these chemical shifts (52.7 and 172 ppm, respectively) are located upfield by ca. 4−5 ppm relative to those for the α-helical conformations.[2,43] Figure 10 provides assignments for the other peaks; Table 3 summarizes the data. Because the amide C═O resonance in the β-sheet conformation partially overlaps with the signal from the side-chain ester moiety, distinctions between the two peptide secondary structures are best performed from the distinctly different C_α resonances (57.5 ppm for α-helices, 52.7 ppm for β-sheets).[2]

Figure 11 presents scale-expanded (C═O and C_α regions) solid-state NMR spectra of phenolic/PMLG, phenolic/PELG, and phenolic/PBLG blends at the same composition of phenolic resin (40 wt %), recorded at room temperature. From the C_α region of the spectrum of the phenolic/PMLG blend system, the content of α-helical conformations was almost identical to that of pure PMLG; in the phenolic/PELG and phenolic/PBLG systems, however, the contents of α-helical conformations were greater than those of the pure PELG and PBLG homopolymers. In addition, a new peak

appeared at ca. 173−174 ppm (downfield to the signals of both the C═O groups and β-sheet of the polypeptides) in the C═O region of the spectra for all three blends, presumably representing the hydrogen-bonded C═O groups.[68,69] The contribution of a second signal related to the hydrogen-bonded C═O group. All of these results are consistent with the features determined from the FTIR spectra.

We obtained additional information regarding the structures of the phenolic/PMLG, phenolic/PELG, and phenolic/PBLG blends from their proton relaxation behavior. We measured the spin−lattice relaxation time in the rotating frame $T_{1\rho}{}^{H}$ to examine the homogeneity of the polymer blends on the molecular scale. The magnetization of resonance is expected to decay according to the exponential function model

$$M_\tau = M_0 \exp(-\tau/T_{1\rho}(H))$$

where τ is the delay time used in the experiment and M_τ is the corresponding peak intensity. The value of $T_{1\rho}{}^{H}$ can be obtained from the slope of the plot of $\ln(M_\tau/M_0)$ with respect to τ. Figure 12 displays the $T_{1\rho}{}^{H}$ relaxation behaviors of each of the three blends (monitoring the phenolic signal at 115 ppm). A single value of $T_{1\rho}{}^{H}$ appeared for the blends, indicating their good miscibility and dynamic homogeneity. The maximum diffusive path length L can be estimated using the approximate expression

$$\langle L^2 \rangle = 6DT_i$$

For a value of $T_{1\rho}{}^{H}$ of 10 ms and an effective spin diffusion coefficient, D, of 10^{-16} m^2 s^{-1}, the dimensions of the features in the phenolic/PMLG, phenolic/PELG, and phenolic/PBLG blends were less than 2−3 nm in the amorphous phase, consistent with the results from DSC analyses.[62,63,70]

Figure 13 presents FTIR spectra of the phenolic/PMLG, phenolic/PELG, and phenolic/PBLG blends measured at temperatures ranging from 25 to 150 °C. The C═O stretching frequency of each polypeptide split into two bands, one at 1734−1741 cm^{-1} and the other at 1710−1720 cm^{-1}, corresponding to free and hydrogen-bonded C═O groups, respectively. The intensity of the signal for the hydrogen-bonded C═O groups of the polypeptides decreased upon increasing the temperature, as would be expected.[55−58,70] In the phenolic/PMLG = 40/60 blend, the content of β-sheet conformations increased upon increasing the temperature, in agreement with previous observations; the oligopeptide almost exclusively adopted the α-helical conformation at 25 °C.[20,71] In the phenolic/PELG = 60/40 blend, however, the fraction of α-helical conformations decreased upon increasing the temperature from 25 to 75 °C, increased upon increasing the temperature from 75 to 125 °C, and then decreased upon increasing the temperature from 125 to 150 °C. More interestingly, the fraction of α-helical conformations increased upon increasing the temperature in the phenolic/PBLG = 40/60 blend. This trend is the exact opposite of that observed for the phenolic/PMLG blend system. Figure 14 plots the fractions of α-helical conformations in the phenolic/PMLG, phenolic/PELG, and phenolic/PBLG blends with respect to the temperature. The fraction of the α-helical conformations decreased significantly upon heating each of the pure PMLG, PELG, and PBLG oligomers. At a relatively high phenolic content, the phenolic resin appears to stabilize the α-helical conformation at higher temperature, especially in the phenolic/PBLG blend system; however, the fractions of α-helical conformations in the phenolic/PMLG and phenolic/PELG blend systems strongly correlated with the phenolic resin content and temperature. Similar to the results in Figure 9, the stronger hydrogen-bonding interactions in the phenolic/PELG blend than in the phenolic/PMLG blend caused PELG to more readily transform to a greater fraction of α-helical conformations at a relative lower phenolic content upon increasing the temperature. The increased fraction of α-helical conformations upon increasing the temperature at relatively high phenolic contents in all three blend systems may have arisen from disruption of the intermolecular hydrogen bonding between the C═O groups of the polypeptides and the phenolic resin and subsequent enhanced intramolecular hydrogen bonding of the polypeptides. We also recorded FTIR spectra of a polystyrene/PBLG = 60/40 blend—where hydrogen bonding cannot occur between the PS and PBLG segments—at different temperatures (Figure S3). Clearly, the fraction of α-helical conformations decreased significantly upon heating, different from the behavior of the phenolic/PBLG system. This observation confirms that the phenolic resin stabilized the α-helical conformations through hydrogen-bonding interactions upon increasing the temperature.

CONCLUSIONS

We have synthesized three different polypeptide oligomers through ROP of NCA monomers using butylamine as the initiator; we then blended these polypeptides with phenolic resin to induce changes in their secondary structures. DSC and solid-state NMR spectroscopic analyses revealed that each blend system was completely miscible in an amorphous phase over the entire range of compositions. Using the Painter−Coleman association model to analyze the data from the FTIR spectra, the strength of the hydrogen-bonding interactions increased in the order phenolic/PELG > phenolic/PMLG > phenolic/PBLG blends. The fraction of α-helical conformation in these three blend systems correlated strongly with the rigidity of their side-chain groups, the intermolecular hydrogen bonding strength with the phenolic resin, the composition of phenolic resin blend, and the temperature.

ASSOCIATED CONTENT

Supporting Information. Additional characterization data (Figures S1−S3). This material is available free of charge via the Internet at http://pubs.acs.org.

AUTHOR INFORMATION

Corresponding Author

*E-mail: kuosw@faculty.nsysu.edu.tw. Tel: 886-7-5254099.

ACKNOWLEDGMENT

This study was supported financially by the National Science Council, Taiwan, Republic of China, under Contracts NSC 100-2221-E-110-029-MY3 and NSC100-2628-E-110-003.

REFERENCES

(1) Klok, H. A.; Lecommandoux, S. *Adv. Mater.* **2001**, *13*, 1217.
(2) Papadopoulous, P.; Floudas, G.; Klok, H. A.; Schnell, I.; Pakula, T. *Biomacromolecules* **2004**, *5*, 81.
(3) Flory, P.J . *Proc. R. Soc. London, Ser. A* **1956**, *234*, 73.
(4) Yang, J. T.; Doty, P. *J. Am. Chem. Soc.* **1957**, *79*, 761.
(5) Perutz, M. F. *Nature* **1951**, *167*, 1053.

(6) Robinson, C.; Ward, J. C. *Nature* **1957**, *180*, 1183.
(7) Yu, S. M.; Conticello, V. P.; Zhang, G.; Kayser, C.; Fournier, M. J.; Mason, T. L.; Tirrell, D. A. *Nature* **1997**, *389*, 167.
(8) Tohyama, K.; Miller, W. G. *Nature* **1981**, *289*, 813.
(9) Prystupa, D. A.; Donald, A. M. *Macromolecules* **1993**, *26*, 1947.
(10) Kuo, S. W.; Lee, H. F.; Chang, F. C. *J. Polym. Sci., Polym. Chem.* **2008**, *46*, 3108.
(11) Blondelle, S. E.; Forood, B.; Houghten, R. A.; Perez-Paya, E. *Biochemistry* **1997**, *36*, 8393.
(12) Gitsas, A.; Floudas, G.; Mondeshki, M.; Spiess, H. W.; Aliferis, T.; Iatrou, H.; Hadjichristidis, N. *Macromolecules* **2008**, *41*, 8072.
(13) Sanchez-Ferrer, A.; Mezzenga, R. *Macromolecules* **2010**, *43*, 1093.
(14) Zhou, Q. H.; Zheng, J. K.; Shen, Z. H.; Fan, X, H.; Chen, X. F.; Zhou, Q. F. *Macromolecules* **2010**, *43*, 5367.
(15) Lee, H. F.; Sheu, H. S.; Jeng, U. S.; Huang, C. F.; Chang, F. C. *Macromolecules* **2005**, *38*, 6551.
(16) Papadopoulos, P.; Floudas, G.; Schnell, I.; Aliferis, T.; Iatrou, H.; Hadjichristidis, N. *Biomacromolecules* **2005**, *6*, 2352.
(17) Rao, J.; Zhang, Y.; Zhang, J.; Liu, S. *Biomacromolecules* **2008**, *9*, 2586.
(18) Ibarboure, E.; Papon, E.; Rodriguez-Hernandez, J. *Polymer* **2007**, *48*, 3717.
(19) Ibarboure, E.; Rodriguez-Hernandez, J. *J. Polym. Sci., Polym. Chem.* **2006**, *44*, 4668.
(20) Klok, H. A.; Langenwalter, J. F.; Lecommandoux, S. *Macromolecules* **2000**, *33*, 7819.
(21) Lecommandoux, S.; Achard, M. F.; Langenwalter, J. F.; Klok, H. A. *Macromolecules* **2001**, *34*, 9100.
(22) Crespo, J. S.; Lecommandoux, S.; Borsali, R.; Klok, H. A.; Soldi, V. *Macromolecules* **2003**, *36*, 1253.
(23) Papadopoulos, P.; Floudas, G.; Schnell, I.; Lieberwirth, I.; Nguyen, T. Q.; Klok, H. A. *Biomacromolecules* **2006**, *7*, 618.
(24) Klok, H. A.; Lecommandoux, S. *Adv. Polym. Sci.* **2006**, *202*, 75.
(25) Floudas, G.; Papadopoulos, P.; Klok, H. A.; Vandermeulen, G. W. M.; Rodriguez-Hernandez, J. *Macromolecules* **2003**, *36*, 3673.
(26) Ibarboure, E.; Papon, Z. E.; Rodriguez-Herna, J. *Polymer* **2007**, *48*, 3717.
(27) Kang, I. K.; Ito, Y.; Sisido, M.; Imanishi, Y. *Biomaterials* **1988**, *9*, 349.
(28) Hua, C.; Dong, C. M.; Wei, Y. *Biomacromolecules* **2009**, *10*, 1140.
(29) Huang, C. J.; Chang, F. C. *Macromolecules* **2008**, *41*, 7041.
(30) Perly, B.; Douy, A.; Gallot, B. *Makromol. Chem.* **1976**, *177*, 2569.
(31) Nakajima, A.; Hayashi, T.; Kugo, K.; Shinoda, K. *Macromolecules* **1979**, *12*, 840.
(32) Yoda, R.; Komatsuzaki, S.; Hayashi, T. *Biomaterials* **1995**, *16*, 1203.
(33) Tomoya, H.; Rudolf, F. *React. Funct. Polym.* **2009**, *69*, 429.
(34) Kong, X.; Jenekhe, S. A. *Macromolecules* **2004**, *37*, 8180.
(35) Kuo, S. W.; Lee, H. F.; Huang, W. J.; Jeong, K. U.; Chang, F. C. *Macromolecules* **2009**, *42*, 1619.
(36) Kuo, S. W.; Tsai, H. T. *Polymer* **2010**, *51*, 5605.
(37) Lin, Y. C.; Kuo, S. W. *J. Polym. Sci., Polym. Chem.* **2011**, *49*, 2127.
(38) Painter, P. C.; Tang, W. L.; Graf, J. F.; Thomson, B.; Colema, M. M. *Macromolecules* **1991**, *24*, 3929.
(39) Asano, A.; Kurotu, T. *J. Mol. Struct.* **1998**, *441*, 129.
(40) Murata, K.; Katoh, E.; Kuroki, S.; Ando, I. *J. Mol. Struct.* **2004**, *689*, 223.
(41) Deng, X.; Hao, J.; Yuan, M.; Xiong, C.; Zhao, S. *Polym. Int.* **2001**, *50*, 37.
(42) Aoi, K.; Nakamura, R.; Okada, M. *Macromol. Chem. Phys.* **2000**, *201*, 1059.
(43) Floudas, G.; Spiess, H. W. *Macromol. Rapid Commun.* **2009**, *30*, 278.
(44) Coleman, M. M.; Graf, J. F.; Painter, P. C. *Specific Interactions and the Miscibility of Polymer Blends*; Technomic Publishing: Lancaster, PA, 1991.
(45) Daly, W. H.; Poche, D. *Tetrahedron Lett.* **1988**, *29*, 5859.
(46) Lin, H. C.; Kuo, S. W.; Huang, C. F.; Chang, F. C. *Macromol. Rapid Commun.* **2006**, *27*, 537.
(47) Agut, W.; Taton, D.; Lecommandoux, S. *Macromolecules* **2007**, *40*, 5653.
(48) Agut, W.; Agnaou, R.; Lecommandoux, S.; Taton, D. *Macromol. Rapid Commun.* **2008**, *29*, 1147.
(49) Xiao, C.; Zhao, C.; He, P.; Tang, Z.; Chen, X.; Jing, X. *Macromol. Rapid Commun.* **2010**, *31*, 991.
(50) Lodge, T. P.; Mcleish, T. C. B. *Macromolecules* **2000**, *33*, 5278.
(51) Papadopoulos, P.; Floudas, Schnell, I.; Klok, H. A.; Aliferis, T.; Iatrou, H.; Hadjichristidis, N. *J. Chem. Phys.* **2005**, *122*, 224906.
(52) Huang, C. F.; Kuo, S. W.; Lin, F. J.; Huang, W. J.; Wang, C. F.; Chen., W. Y.; Chang, F. C. *Macromolecules* **2006**, *39*, 300.
(53) Kuo, S. W.; Chan, S. C.; Chang, F. C. *Macromolecules* **2003**, *36*, 6653.
(54) Kuo, S. W.; Huang, C. F.; Chang, F. C. *J. Polym. Sci., Polym. Phys.* **2001**, *39*, 1348.
(55) Kuo, S. W. *J. Polym. Res.* **2008**, *15*, 459.
(56) He, Y.; Zhu, B.; Inoue, Y. *Prog. Polym. Sci.* **2004**, *29*, 1021.
(57) Coleman, M. M.; Painter, P. C. *Prog. Polym. Sci.* **1995**, *20*, 1.
(58) Coleman, M. M.; Painter, P. C. In *Polymer Blend*; Paul, D. R., Bucknall, C. B., Eds.; Wiley: New York, 2000.
(59) Surewicz, W. K.; Mantsch, H. H. *Biochim. Biophys. Acta* **1988**, *952*, 115–130.
(60) Ma, C. C. M.; Wu, H. D.; Peter, P. C.; Han, T. T. *Macromolecules* **1997**, *30*, 5443.
(61) Jeon, S.; Choo, J.; Sohn, D.; Lee, S. N. *Polymer* **2001**, *42*, 9915.
(62) Kuo, S. W.; Chang, F. C. *Macromol. Chem. Phys.* **2002**, *203*, 868.
(63) Kuo, S. W.; Chang, F. C. *Macromolecules* **2001**, *34*, 4089.
(64) Kuo, S. W.; Chang, F. C. *Macromolecules* **2001**, *34*, 5224.
(65) Kuo, S. W.; Tung, P. H.; Chang, F. C. *Macromolecules* **2006**, *39*, 9388.
(66) Murata, K.; Katoh, E.; Kuroki, S.; Ando, I. *J. Mol. Struct.* **2004**, *689*, 223.
(67) Kricheldorf, H. R.; Muller, D. *Macromolecules* **1983**, *16*, 615.
(68) Huang, M. W.; Kuo, S. W.; Wu, H. D.; Chang, F. C.; Fang, S. Y. *Polymer* **2002**, *43*, 2479.
(69) Hill, D. J. T.; Whittaker, A. K.; Wong, K. W. *Macromolecules* **1999**, *32*, 5285.
(70) Coleman, M. M.; Painter, P. C. *Miscible Polymer Blend-Background and Guide for Calculations and Design*; DEStech Publications Inc.: Lancaster, PA, 2006.
(71) Abraham, S.; Ha, C. S.; Kim, I. *J. Polym. Sci., Polym. Chem.* **2006**, *44*, 2774.